A Library of Tunable Agarose Carbomer-Based Hydrogels for Tissue Engineering Applications: The Role of Cross-Linkers

Filippo Rossi,[1] Giuseppe Perale,[1] Giuseppe Storti,[2] Maurizio Masi[1]

[1]*Department of Chemistry, Materials and Chemical Engineering ''Giulio Natta'', Politecnico di Milano, Via Mancinelli 7, 20131 Milano, Italy*
[2]*Institute for Chemical and Bioengineering, ETH Zurich, Campus Hoenggerberg, HCI F125, Wolfgang Pauli Str. 10, 8093 Zurich, Switzerland*

Received 11 October 2010; accepted 4 April 2011
DOI 10.1002/app.34731
Published online 23 August 2011 in Wiley Online Library (wileyonlinelibrary.com).

ABSTRACT: The role of the crosslinking agents was studied for a series of agarose–carbomer-based hydrogels, specifically developed for tissue engineering applications, and was quantified using the most typical polycondensation parameter; the ratio between the reacting moieties, i.e., hydroxyl (*A*) and carboxyl (*B*) groups. Because of the bonds among hydrophilic groups, as *A/B* ratio was increased, the gel network showed higher compactness and less ability to swell. The role of crosslinkers was also further analyzed using environmental scanning electron microscopy (E/SEM) and rheological measurements. SEM analysis underlined the presence of different structures as well as the erosion due to the presence of cosolvents in hydrogel synthesis. Rheological measurements showed the dependence of crossover strain value and yield stress upon the ratio of hydroxyl/carboxyl groups and, generally, a clear pseudoplastic behavior. Such detailed characterizations were essential to investigate the design of an optimized formulation capable of being a proper hosting environment for glial cells, which were here used as they are a promising cell type in several central nervous system repair strategies. © 2011 Wiley Periodicals, Inc. J Appl Polym Sci 123: 2211–2221, 2012

Key words: hydrogels; polycondensation; rheology; swelling

INTRODUCTION

Tissue engineering, briefly the smart combination of cells and materials to replace damaged or missing parts of living tissues, is widely accepted as being the future in medicine and health care.[1–3] Recent highlights[4] suggest the combined use of cells and materials together also with specific, and appropriate active agents (drugs, antibodies, peptides).[5,6] Among all known and used materials,[7–9] emerging strategies of the last few years[4,10] confirm a very strong interest in hydrogel as great candidates for both cell housing and drug delivery,[11–14] allowing to build water-based systems with cells directly included inside gel and drugs solved within the water contained in the polymeric network.[12,15]

Hydrogels are three dimensional networks of hydrophilic polymers linked together by chemical bonds, such as covalent bonds, and cohesive forces, like hydrogen bridges, ionic bonds, or hydrophobic associations.[8,10,11] Generally, being hydrogels obtained by random walk reactions, the three most typical parameters for their characterization are the following: (1) the network mesh size expressed in nm, ζ, (2) the number average molecular weight between two following crosslinks, M_C, in g mol^{-1} and (3) the crosslinking density, ν, in mol cm^{-3}.[16,17]

In general their high adaptability makes hydrogel extremely suitable for different medical needs, but the possibility to use a large amount of monomers and reagents could be very critical and expensive, especially from an industrial point of view. Hence, the study and development of a unique tunable library synthesized starting from the same reaction system could be the winning point.[18,19] Moreover, the possibility to address different medical applications, maintaining the same polymeric skeleton, facilitates chemical and material studies on one side and reduces costs on the other.

This present work, indeed, regards a library of hydrogels (here briefly indicated with the ACn acronyms) synthesized by copolymerization between two polymers. The first being agarose,[20] a commonly used natural polysaccharide, while the second being carbomer 974P,[21] a highly branched synthetic polyacrylic acid commonly used in its aqueous solution for ophthalmic applications. As well known, the combined use of both natural and synthetic polymers appears to be a good combination to enhance biocompatibility on one side and designing possibilities on the other.[4,22] Previous investigations proved

Correspondence to: Dr. G. Perale (giuseppe.perale@polimi.it).

TABLE I
Composition of Agarose-Carbomer Hydrogels and Hydroxyl (A) Versus Carboxyl (B) Group Ratios (*A*/*B*) for AC Hydrogel Samples

Hydrogel components	AC1	AC2	AC3	AC4	AC5	AC6
PBS (mL)	99.5	99	98.2	97.5	95.5	68.5
Carbomer 974P (g)	0.5	0.5	0.5	0.5	0.5	0.5
Propylene glycol (mL)	0	0	0.3	0	3	30
Glycerol (mL)	0	0.5	1	2	1	1
Triethylamine (mL)	0.5	0.5	0.5	0.5	0.5	0.5
Agarose (g)	0.25	0.25	0.25	0.25	0.25	0.25
A/B	2	10	11	20	40	100

that this kind of hydrogels are promising 3D scaffold for cell housing, particularly for cells of the central nervous system (CNS) and stem cells,[23,24] and carrier for pharmacological treatments.[12,25]

Here, starting from swelling kinetics, the characteristic Flory-Rehner parameters were evaluated and then gel morphology and rheological properties were studied considering crosslinkers' role.[16] The ability to carry cells was analyzed with respect to hydroxyl/carboxyl groups ratio, to underline the tuning possibilities that make agarose–carbomer hydrogels an extremely adaptable material library for tissue engineering applications.

MATERIALS AND METHODS

Materials

The materials used were: carbomer 974P (MW = 1 MDa, CAS 151687-96-6, Fagron, The Netherlands), triethyl-amine (alias TEA, CAS 121-44-8, high purity preparation by Sigma-Aldrich, Germany), propylene glycol (CAS 57-55-6, by Sigma-Aldrich, Germany), glycerol (CAS 56-81-5, by Merck Chemicals, Germany), and agarose (MW = 200 KDa, CAS 9012-36-6, by Invitrogen Corp.). The solvent utilized in this work is PBS, Dulbecco's phosphate-buffered saline solution by ς-Aldrich (pH = 7.4). All materials were used as received.

Hydrogel synthesis

Hydrogels were prepared by bulk reaction in phosphate buffered saline solution (PBS)[26] at about 80°C, where polymeric solution was achieved by stirring polymer into the selected solvent, adding a mixture of crosslinking agents primarily made of propylene glycol and glycerol [along with triethyl-amine (TEA) for pH neutralization]. Reaction pH was indeed kept neutral. Effective gelation and reticulation were achieved by microwave heating for 1 min per 10 mL of polymeric solution.[27] The key parameter to tune the formulation was the amount of free hydroxyl groups. Mixing reactor was kept closed to avoid any eventual loss of solvent vapors and the gelation was achieved in a 48 multiwell cell culture plate (0.5 mL each and with the cylinder diameter of 1.1 cm) where the gelling solution was poured during cooling. The hydrogel compositions of the tested formulations are collected in Table I, which also presents the hydroxyl versus carboxyl groups ratios (A/B values).

The library was investigated by experimental analysis on six different gels having as differences only the crosslinkers concentrations: propylene glycol with a 0 : 1 : 10 : 100 ratio while glycerol with a 0 : 1 : 2 one (as can be seen from Table I). Proportions used were indeed chosen to allow a deep understanding of each component effect on gel structure and thus on macroscopic gel behavior.[15,28]

The stability of those materials is quite high; they remain stable for weeks before significant degradation, by hydrolysis,[29] takes place. Since such characteristic time is much larger than the experimental time, degradation reactions are fully neglected in this work.

Physical characterization

Fourier transform-infrared (FT-IR) spectra

Hydrogel samples, after being left to soak for 24 h in excess of solvent, were freeze-dried and laminated with potassium bromide. FT-IR spectra were recorded within the polymeric network using a Thermo Nexus 6700 spectrometer coupled to a Thermo Nicolet Continuum microscope equipped with a 15× Reflachromat Cassegrain objective.

Measurement of swelling kinetics and equilibrium

The hydrogel samples were first immersed in PBS for about 24 h, then freeze-dried, weighed (W_d), and poured in excess PBS to achieve complete swelling at 37°C in 5% CO_2 atmosphere.[30] The swelling kinetics was measured gravimetrically. The samples were removed from PBS at regular time points. Hydrogel surfaces were then gently wiped with moistened filter paper to remove the excess of solvent and then weighed (W_t). Swelling ratio is defined as follows:

$$\text{Swelling ratio} = \frac{W_t}{W_d} \times 100, \quad (1)$$

where W_t is the weight of the wet hydrogel as a function of time and W_d that of the dry hydrogel as evaluated after freeze-drying.[15,28,31] The equilibrium of swelling is the plateau value reached by the kinetics.[15]

Flory-Rehner theory

According to the Flory-Rehner description, as said, swelling data can be used to evaluate some important structural parameters of the hydrogel such as: (a) mean mesh size ζ (nm), (b) average molecular weight between two following crosslinks M_c (g mol^{-1}), (c) mean crosslinkage density ν (mol cm^{-3}).[11,16,32] Using a simplified version of the Flory-Rehner equation,[10,12,16] the average molecular weight M_C was evaluated as a function of the volumetric swelling ratio, $Q_{V,}$ as:

$$Q_V^{5/3} = \frac{V_P \times M_C}{V_1} \times (0.5 - \chi) \quad (2)$$

in this equation, V_p is the specific volume of dry polymer, V_1 the specific volume of the solvent (PBS), and χ the Flory interaction parameter between polymer and solvent obtained from literature.[33–35] Q_V was evaluated from the mass swelling ratio (Q_M) through the following equation:

$$Q_V = 1 + \frac{\rho_p}{\rho_s} \times (Q_M - 1), \quad (3)$$

where ρ_p is the density of the dry polymer, obtained by pycnometry, and ρ_s that of the solvent.

The crosslinking density was determined as[36]:

$$\nu = \frac{\rho_p}{M_C} \quad (4)$$

and the swollen hydrogel mesh size was calculated using the following equation[37]:

$$\zeta = Q_V^{1/3} \times \sqrt{r_0^2} \cong 0.1707 \times (M_C)^{1/2} \times (Q_V)^{1/3} \quad (5)$$

where $\sqrt{r_0^2}$ is the root main square of the end-to-end distance between crosslinks on unperturbed distance considering the most concentrated polymer present that is agarose.[12,34,38]

Polycondensation

According to generally accepted Flory's model, hydrogel synthesis was here studied as a conventional polycondensation; the two condensing groups are the hydroxyl ones (Group A), present in propylene glycol, glycerol, agarose, and carbomer 974P, and the carboxyl groups (Group B) present in carbomer 974P. To evaluate the A/B ratio (presented in Table I), the following equation can be used:

$$\text{Group}_j = \sum_{i=1}^{N} \frac{m_i}{\text{MW}_i} \times f_{ij} \quad (6)$$

In this equation m_i is the mass of the generic ith component (corresponding percentages shown in Table I) MW_i its molecular weight, f_{ij} its functionality[16] with respect to group j and N the number of components containing jth group. If A and B have exactly the same value, there's a perfect balance between carboxyl and hydroxyl groups (stoichiometric formulation). If not, unreacted groups remain at the end of the reaction; the larger the value of A/B is, the larger amount of A unreacted groups. The A/B values for the gel samples studied are presented in Table I.

Morphological studies: Environmental scanning electron microscopy (E/SEM) analysis

Environmental scanning electron microscopy analysis was performed on gold sputtered samples at 10 kV with Evo 50 EP Instrumentation (Zeiss, Jena, Germany). To preserve the actual morphology of the hydrogel under complete swelling, freeze-drying (24 h) was applied to remove all the liquid phase by sublimation. Because of the low operating values of temperature and pressure, the polymer chains were expected to retain the same conformation they had in wet conditions.[15,28] Comparative evaluation of the superficial and internal morphology of two largely different materials was carried out, to understand the dependence of A/B on macro scale; samples AC1 and AC6 were considered because they represent the lower and upper limits, respectively, of the explored A/B ratios range.

Rheological characterization

The rheological behavior was studied at 37°C using a Rheometric Scientific ARES (TA Instruments, New Castle, DE) equipped with parallel plates of 30.0 mm of diameter with a 4-mm gap between them. Room temperature was selected because our materials contain substantial amounts of water and higher temperatures could significantly affect their characteristics, especially at long times. Oscillatory responses (G', elastic modulus, and G'', loss/viscous modulus) were determined at low values of strain (0.02%) over the frequency range 0.1–500 rad s^{-1}.[33,39]

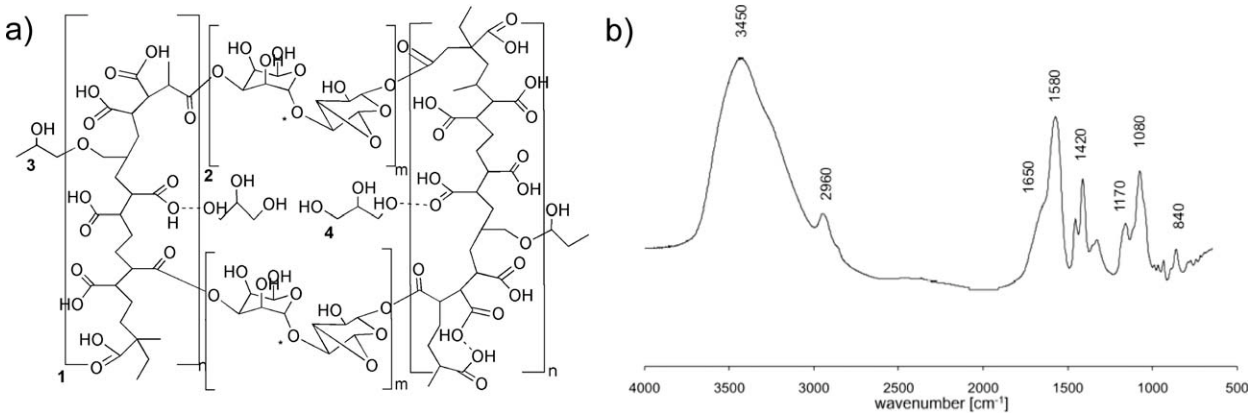

Figure 1 (a) Scheme of the three-dimensional network formed by statistical polycondensation between carbomer 974P (**1**), agarose (**2**) and crosslinking agents [propylene glycol (**3**) and glycerol (**4**)] in phosphate buffer saline solution. Esterification, hydrogen bonding, and carboxylation bring statistically closer the polymer chains, thus creating a stable heterogeneous structure. (b) Fourier transform infrared spectra of AC1 sample. The most important groups in the studied gels are —OH (3450 cm^{-1}), C—H (2960 cm^{-1}), CO_2 (i.e., carboxylates, symmetric around 1560 cm^{-1} and asymmetric around 1420 cm^{-1}), C—N (1080 cm^{-1}), and C—O—C (840 cm^{-1}).

Dynamic Strain Sweep tests were also performed at frequency of 20 rad s^{-1} over the strain range of 0.01–100%. Pseudoplastic behavior was also investigated and the behaviors of shear stress and viscosity as a function of shear rate were examined. The linearity of all viscoelastic properties was verified for all samples.

Standard glial line cell 3D culture

Standard glioma derived U87MG cell line were cultured in Dulbecco's Modified Eagle's Medium (DMEM) supplemented with 10% fetal bovine serum (FBS) (Sigma, Germany), 2 m*M* L-glutamine (Sigma), 100 U mL^{-1} penicillin (Sigma), 0.100 mg mL^{-1} streptomycin (Sigma), 1% sodium pyruvate (Sigma), 1% HEPES buffer (Sigma), at 37°C and 5% CO_2. A solution of suspended cells (density of 0.8×10^4 cells per mL) was added to the gelating samples (at $T = 37$°C) in 1 : 1 volume ratio, and then homogenized into 48-multiwell cell culture plates.[23,24] Each sample of the so obtained biohybrid structures was topped with cell culturing medium and kept in cellular incubator under 5% CO_2 at 37°C. At Day 7, cells were mechanically extracted using a Pasteur pipette with fresh and warm (37°C) medium.[23,26] The obtained cell suspension (100 μL) was diluted at the 1 : 1 ratio using the Trypan Blue (CAS 72-57-1, Sigma, Germany) staining solution and live cells were counted by a hematocytometer.[23,26,40]

Statistical analysis

Experimental data were analyzed using Analysis of Variance (ANOVA). Statistical significance was set to P value ≤ 0.05. Results are presented as mean value ± standard deviation.[41]

RESULTS AND DISCUSSION

Physical characterization

The polycondensation reaction[25] between high molecular weight branched polyacrylic acid (carbomer 974P) and agarose was microwave assisted to obtain a chemically crosslinked hydrogel, as verified with FT-IR analysis (Fig. 1).[12] The solvent used was phosphate buffered solution and its role in hydrogel chemistry was already described.[26] Briefly, being carbomer 974 P high pH-sensitive,[26] the buffered nature of the solvent allowed the possibility to control and tune the reaction. Moreover, its relevant role was observed also with respect to cell housing inside such hydrogels; living cell counts showed higher amount of cells surviving the latency period of inclusion in hydrogel when PBS was used as solvent, while only very few of them survived in a deionized water based gel.[26] Hence, PBS role both in fine control of hydrogel preparation and in material tuning is essential; this latter being a feature of primary importance when applying hydrogels as cell carriers in regenerative medicine applications.

Before polymeric solution irradiation, polymer chains are not overlapped and segmental mobility is high. Increasing irradiation doses, intramolecular links and chain scissions are favored. Thereby the decrease of segmental mobility, allows intermolecular crosslinks to be formed and thus give origin to local 3D networks, also known as "microgels." The further irradiation increase privileged intermolecular crosslinking and chain scission, giving origin to macroscopic gels.[11] In general, chemical interactions would statistically bring polymer chains together and, indeed, the formation of a stable structure occurs through junction zones between chains [scheme in Fig. 1(a)]. The presence of hydroxyl

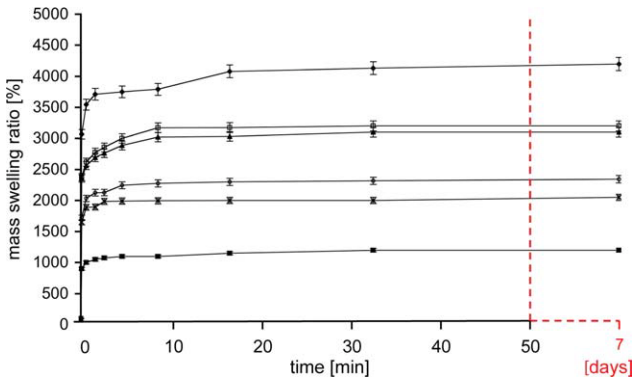

Figure 2 Swelling kinetic of the hydrogels with different amounts of crosslinkers in PBS at 37°C of AC1(◆), AC2(□), AC3(▲), AC4(○), AC5(※), AC6(■). The equilibrium was reached in the first hour and maintained for 7 days. [Color figure can be viewed in the online issue, which is available at wileyonlinelibrary.com.]

groups and carboxyl ones suggests that main interactions occur via esterification and hydrogen bonding (chemical hydrogel), as confirmed by FT-IR analysis [Fig. 1(b)].[12] The esterification takes place between carbomer 974P and either agarose or glycerol or propylene glycol and PBS salts freely solvated in water cause salt carboxylates formation. Moreover, the presence of propylene glycol and glycerol is necessary not only to increase crosslinking possibilities but it also influences solvent viscosity. As explained above, microgels formation is due to segmental mobility that decreases as the solvent viscosity, in which polymers are dissolved, increases. Thus, tuning solvent viscosity shorter-range bonds (high viscosity) or longer-range bonds (low viscosity) can be tailored. Figure 1(b) shows the FT-IR spectra of AC1 gel; the spectrum shows a broad peak of around 3450 cm^{-1}, which is due to the stretching vibration of O—H bonds, while peaks around 2960 cm^{-1} are due to the C—H stretch. The formation of esteric bonds is visible by peaks corresponding to symmetric (around 1560 cm^{-1}) and asymmetric (around 1420 cm^{-1}) CO_2 stretches. Moreover, peaks around 1080 cm^{-1} are related to C—N vibration, confirming the presence of TEA inside the network. Spectra also show peaks related to C—O—C stretch vibration (840 cm^{-1}) which represents the glycosidic bond between two following monosaccharide units (typical of agarose structure).

Because of these reactions, AC hydrogels are quite anionic and this electrostatic nature, confirmed by mass equilibrium swelling at different pH,[26] influences the ability and the kinetics involved in drug delivery.[12] AC hydrogels can be rightfully considered a "material library" where dissimilarities lie in different amount of crosslinkers involved in polycondensation, identified and briefly described through the ratio between hydroxyl and carboxyl groups (A/B) in Table I. AC6 presents a higher A/B ratio, which affects not only its microchemistry but also its physical properties, oppositely to what happens on AC1.

The ability to absorb and retain water, within their 3D polymeric network, is the key feature for a hydrogel system; swelling is thus the first characteristic to investigate. Figure 2 shows the swelling kinetic and the equilibrium of the hydrogel samples with different amount of crosslinkers in PBS at 37°C and 5% CO_2 atmosphere. All samples exhibited fast swelling kinetics and they reached equilibrium of swelling within the first hour maintaining this state for a week[29] (values presented in Table II) before the start of hydrolytic degradative reactions. Compared to the hydrogels with larger amounts of crosslinkers (A/B ratio in Table I), the hydrogels with smaller amounts of A groups exhibited higher values of swelling equilibrium. The differences experimentally observed are due to a higher ability to retain water when the amount of crosslinkers is smaller. However, increasing A/B ratio, water molecules cannot easily diffuse into the hydrogel network, making the hydrogel network denser with consequent reduced volumetric expansion.

When a polymeric network is swollen, its chains achieve an elongated conformation; such elongation is contrasted by an opposite elastic force, thus limiting chains stretching on one hand. On the other hand, the polymer-solvent mixing increases the system entropy, thus favoring the hydrogel swelling toward lower free energy configurations. At equilibrium, such opposite forces are balanced and the maximum swelling extent is achieved. Starting from these statements described by Flory-Rehner theory several hydrogel features, such as ζ, M_c, and ν, can be readily evaluated following the simplified Flory-Rehner eqs. (2)–(5). Estimated values of these three parameters are summarized in Table II for all the examined hydrogel samples, along with the corresponding equilibrium swelling ratio (1) values.

The effect of crosslinkers was to make more compact the hydrogel structure; as a matter of fact, estimated mesh sizes decreased from 90 nm (AC1) to 28 nm (AC6). Moreover, if an increase in mesh size

TABLE II
Physical Characteristics for Hydrogel Samples

Samples	Swelling equilibrium (%)	ζ (nm)	M_c (g/mol)	ν (μmol/cm^3)	t^* (min)
AC1	4500	90	15540	113	16.6
AC2	3200	61	8735	200	8.6
AC3	3100	59	8300	210	8.6
AC4	2350	42	5210	334	4.6
AC5	2050	36.5	4280	407	2.6
AC6	1200	28	3450	506	1.6

is considered, a decrease in crosslinking density and an increase in molecular weight M_c are consequently found. Indeed, in hydrogels with higher mesh size values, two following crosslinks are further from each other; therefore, the molecular weight between two following crosslinks is higher and crosslinking density correspondingly lower. The crosslinkers involved in this polycondensation were propylene glycol and glycerol; they play the role of —OH sources but they are also responsible for the increase in system viscosity, propylene glycol specifically. On one side their influence on final physical properties depends on their functionalities f.[16] An increase on functionality, that is three for glycerol and two for propylene glycol, corresponds to a major effect on the three characteristic structural parameters studied in this work. This is due to the increasing crosslinking possibilities during gelation. On the other side, the viscosity increase due to their presence as cosolvents is responsible of a general reduction in chains mobility inside gelling solution causing; crosslinking reactions to occur on a shorter range, self crosslinking along carbomer chains, thus smaller meshes are obtained and, in the end, microgels formation is thus preferably promoted. With reference to A/B ratio, it was useful to deeply examine how crosslinking agents influence physical characteristics. Because of the presence of bonds between the hydrophilic groups, the whole gel network was more compact and less water was absorbed when hydroxyl groups prevailed on carboxyl ones ($A/B \gg 1$). Table II shows that mesh size decreases as A/B increases; as explained above, this trend is fulfilled also by swelling equilibrium values and swelling behavior. Indeed, lower ability to retain water corresponds to lower mesh size and average molecular weight values on one side.

Moreover, the trend of M_c (i.e., average molecular weight between two following crosslinks) is similar to what explained before for mesh size, decreasing from 15,450 to 3445 g mol^{-1}. Similarly, crosslinking density increases as hydroxyl groups prevails on carboxyl ones; a lower ability to absorb water corresponds to a more compact and stiff network.

To summarize, an increase in A/B value corresponds to lower values of mesh size and average molecular weight between two following crosslinks, thus to higher values of crosslinking density. From swelling kinetics presented in Figure 1, it can be noted that hydrogels reached the equilibrium of swelling (plateau) very quickly but with different kinetics; the time needed to establish the equilibrium of swelling, t^*, is shown in Table II as a function of the A/B ratio. As the network is swelling by solvent absorption, the chains between network junctions are stretched, i.e., they assume elongated configurations, and a contrasting force due to rubber elasticity develops in opposition to such process of volume increase. As swelling proceeds, this force increases and an equilibrium situation is finally established. This behavior is fully consistent with the data trends (Table II); by increasing the mesh size, the ability to retain water increases. Contemporaneously, the time needed to reach the equilibrium of swelling, between attractive and repulsive forces, increases due to the bigger distance between polymeric chains. In sample AC6, interconnection forces are larger; as a result, such material hinders water diffusion better than the other samples and equilibrium conditions are achieved very quickly, at small swelling equilibrium values.

Morphological studies (E/SEM)

To preserve the actual morphology of the hydrogel under complete swelling, freeze-drying was applied to remove all the liquid phase by sublimation. Because of the low operating values of temperature and pressure, polymer chains were reasonably expected to retain the same conformation they had in wet conditions.[41] The morphological characterization was carried out on the two "limit" samples, AC1 and AC6.

Figure 3 presents micrographs corresponding to surface (a,b) and internal morphologies (c,d) of AC1 and AC6 samples. From surface micrographs, smooth and glassy morphology is visible for both formulations with high degree of irregularity and heterogeneities. Among them, AC6 exhibits more irregularities due to higher crosslinking degree (A/B) on one side and the presence of cosolvents on the other. As explained above, cosolvents influence bond distance, decreasing polymeric chain mobility during polycondensation. Moreover, both systems seem to be extremely close packed and thick, thus impeding the evaluation of mean pore size. Even if E/SEM cannot show network nano-details such as mesh size for nanostructured materials, sample AC1 exhibits a more defined network structure while AC6 is a more compact and stiff one.

Rheological characterization

Figure 4 shows dynamic frequency sweep test (DFS) spectra performed at 37°C for AC1 and AC6 gel samples. For both formulations storage modulus (G') was found to be approximately one order of magnitude higher than the loss modulus (G''), indicating an elastic rather than viscous material. Furthermore, both G' and G'' are essentially independent from frequency over the entire investigated range, thus indicating dominant viscoelastic relaxations of networks at lower frequency values. This means that network relaxation time, τ, is rather long ($\tau \approx 2000$ s); this

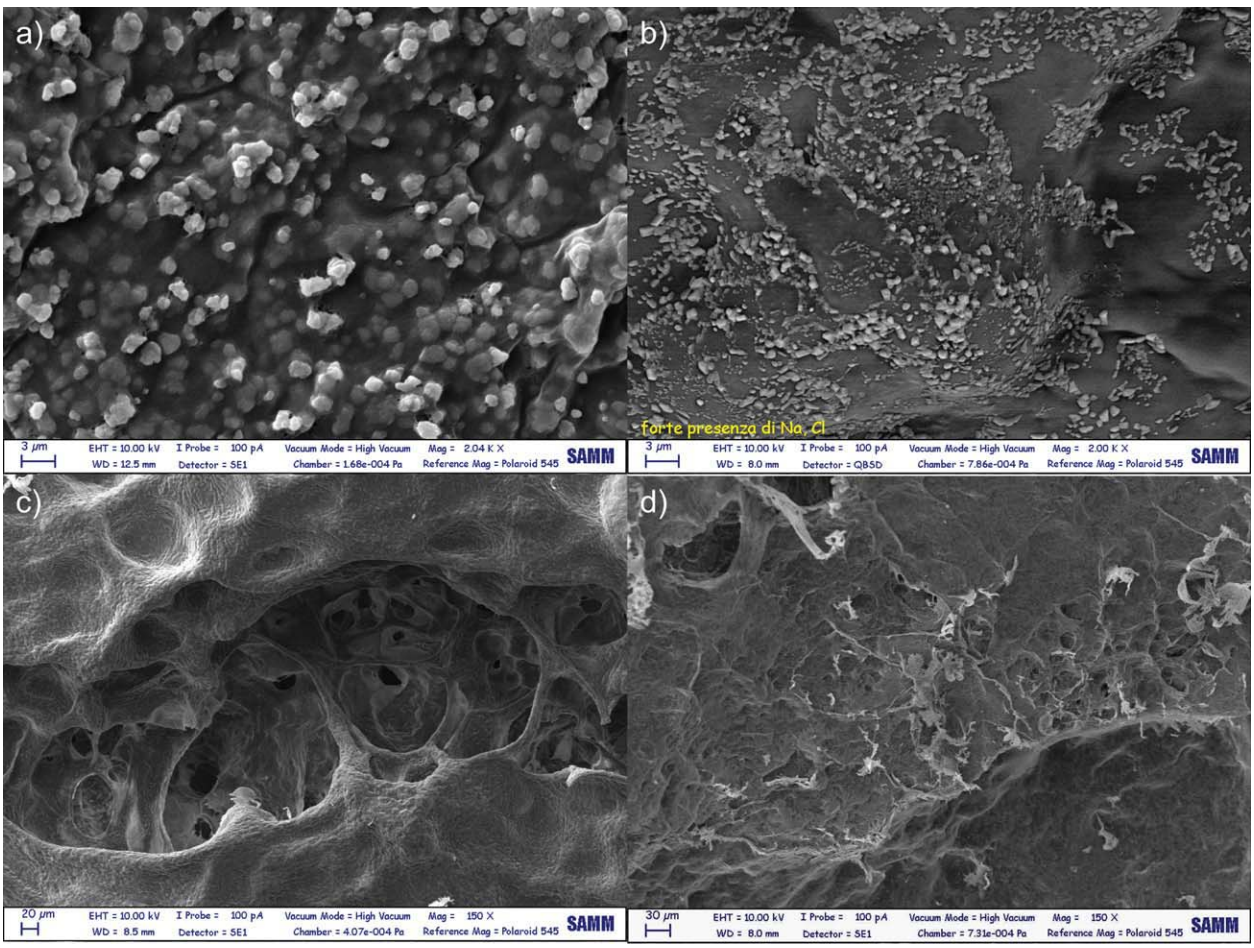

Figure 3 E/SEM micrographs of AC hydrogels. (a, b) surface morphology of AC1 and AC6 samples, respectively, (×2 magnification); (c, d) internal morphology of AC1 and AC6 samples, respectively, (×150 magnification). [Color figure can be viewed in the online issue, which is available at wileyonlinelibrary.com.]

long reorganization time is required by the system to reach complete equilibrium and form a well-defined network structure. This characteristic time is larger than typical values reported for other Carbopol based gels[42] and it is most probably effected by cosolvent system, glycerol–propylene glycol added to PBS; indeed, this system exhibits a much larger viscosity than that of the classical phosphate buffered saline solution. Such rheological behavior matches the characteristic signature of a solid-like gel, confirming this nature for both AC type gels. Moreover, the value obtained for G' (750 Pa for AC6) are of the same order of magnitude as the modulus reported in literature for other biopolymers and hydrogels.[42]

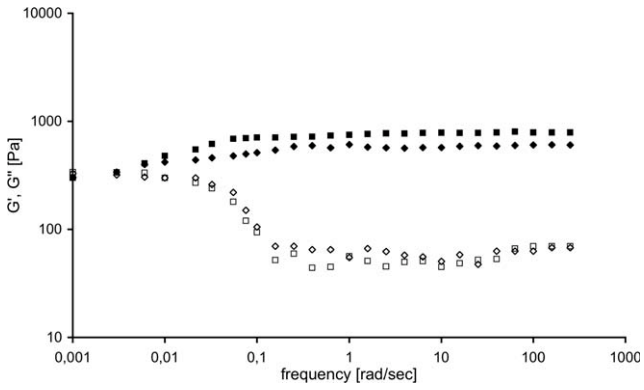

Figure 4 Frequency-dependent properties of AC1 (G' (◆), G'' (◇)) and AC6 (G' (■), G'' (□)) hydrogel samples.

The results of the dynamic strain sweep test (DSS) are shown in Figure 5; it is clearly visible that hydrogel behavior is dominated at low strain values by the elastic modulus.

With the increase of strain values, the elastic structure of the network breaks down and the elastic modulus decreases steeply. The crossover strain (γ_c) can be readily identified as the value at which the contribution of tan(δ) is predominant with respect to G' ($\gamma_c = 0.6$ in AC6 case). The trend of G', at low values of strain, indicates the presence of a close packed polymeric network. In addition, the pseudoplastic behavior of AC samples at high shear rates is presented in Figure 6(a,b).

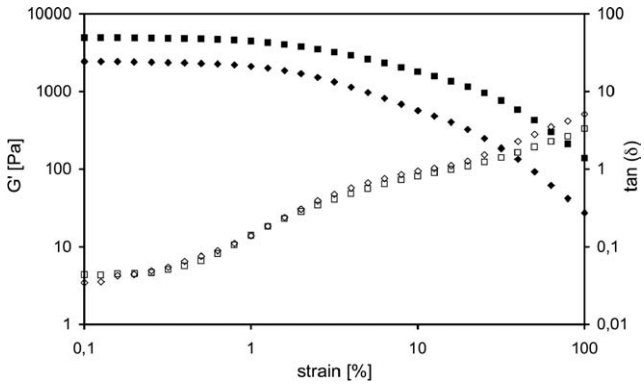

Figure 5 Dynamic strain sweep experiments of AC1 (G' (◆) and tan(δ) (◇)) and AC6 (G' (■) and tan(δ) (□)) at constant frequency.

Moreover, to widen the investigations previously carried out on injectability,[12,25] yield stress can be readily calculated from data in Figure 7. To fulfill the requirements for injectable matrices, yield stress should be high enough to prevent flow out of the container due to sample weight when the container is placed in upside down position. On the other hand, the same stress cannot be too high, because this could cause problems during application and injection.[41] For sample AC6, the value of yield stress as measured by oscillatory sweep test, was ~ 40 Pa (Fig. 7).

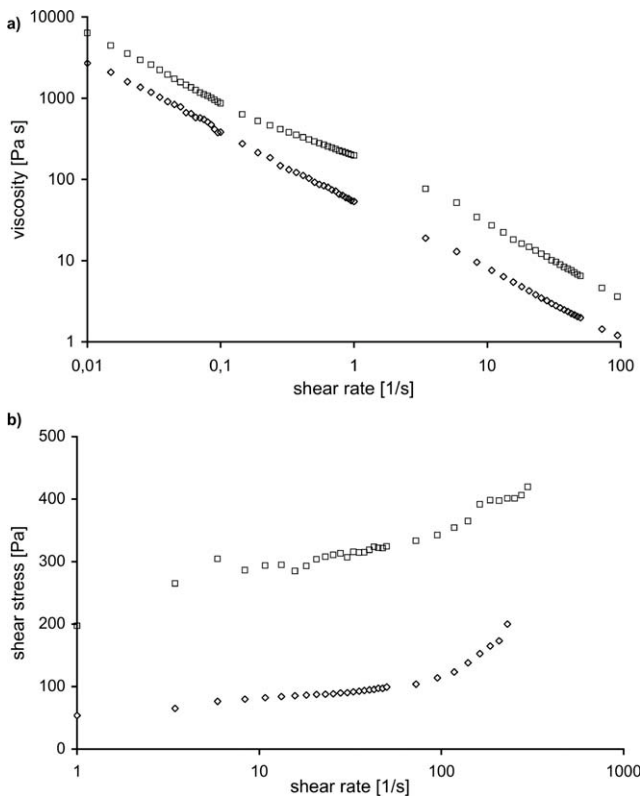

Figure 6 Determination of pseudoplasticity for AC1 (◇) and AC6 (□): (a) viscosity versus shear rate and (b) shear stress versus shear rate.

Rheological characterization: The role of crosslinkers

The dependence of the rheological behavior upon the amount of crosslinker was analyzed again by comparing the results collected with the two limit samples, in terms of A/B ratio, AC1 and AC6, respectively. As expected, AC6 behaves as a more rigid network than AC1 and this is in perfect agreement with structural differences due to the presence of crosslinkers, as also shown by swelling studies.

The data in the same three plots already commented above (dynamic strain sweep experiment, experiment for pseudoplasticity, and oscillatory measurement of yield stress strain) were considered. In Figure 4, the results of the dynamic strain sweep test were shown; for both hydrogel samples, the elastic modulus (G') dominates at low values of strain corresponding to 750 Pa for AC6 and 600 Pa for AC1. Above the crossover strain (γ_c), the contribution of tan(δ) is larger than the elastic one. From the results in Figure 5 it is also evident that crossover strain decreases at increasing A/B ratio (extent of crosslinking), ranging from 0.30 for AC1 to 0.60 for AC6. The values of G' are larger for AC6, which proves the more compact nature of this material and the larger amount of crosslinks. On the other hand, the behaviors of tan(δ) are very similar, thus indicating very similar, liquid-like behaviors. In Figure 6(b), data of viscosity at increasing shear rate are shown demonstrating pseudoplastic behavior; as expected, higher viscosities are found increasing crosslinking density. The last comparison between the two formulations can be done in terms of yield stress (Fig. 7), showing a decrease from AC6 to AC1. Therefore, in terms of crosslinks, an increase in network entanglements corresponds to an increase in strength that must be applied for start flowing.

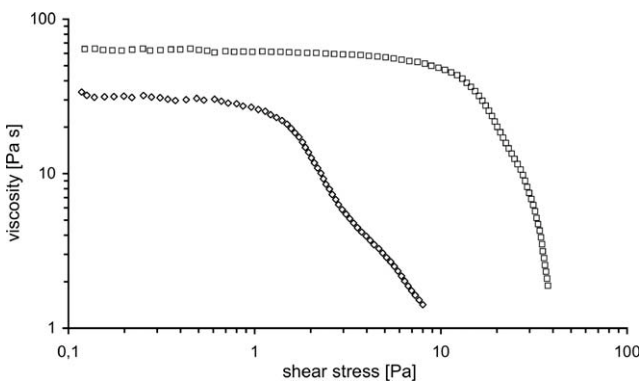

Figure 7 Measure of yield stress of AC1 (◇) and AC6 (□) by oscillatory experiments.

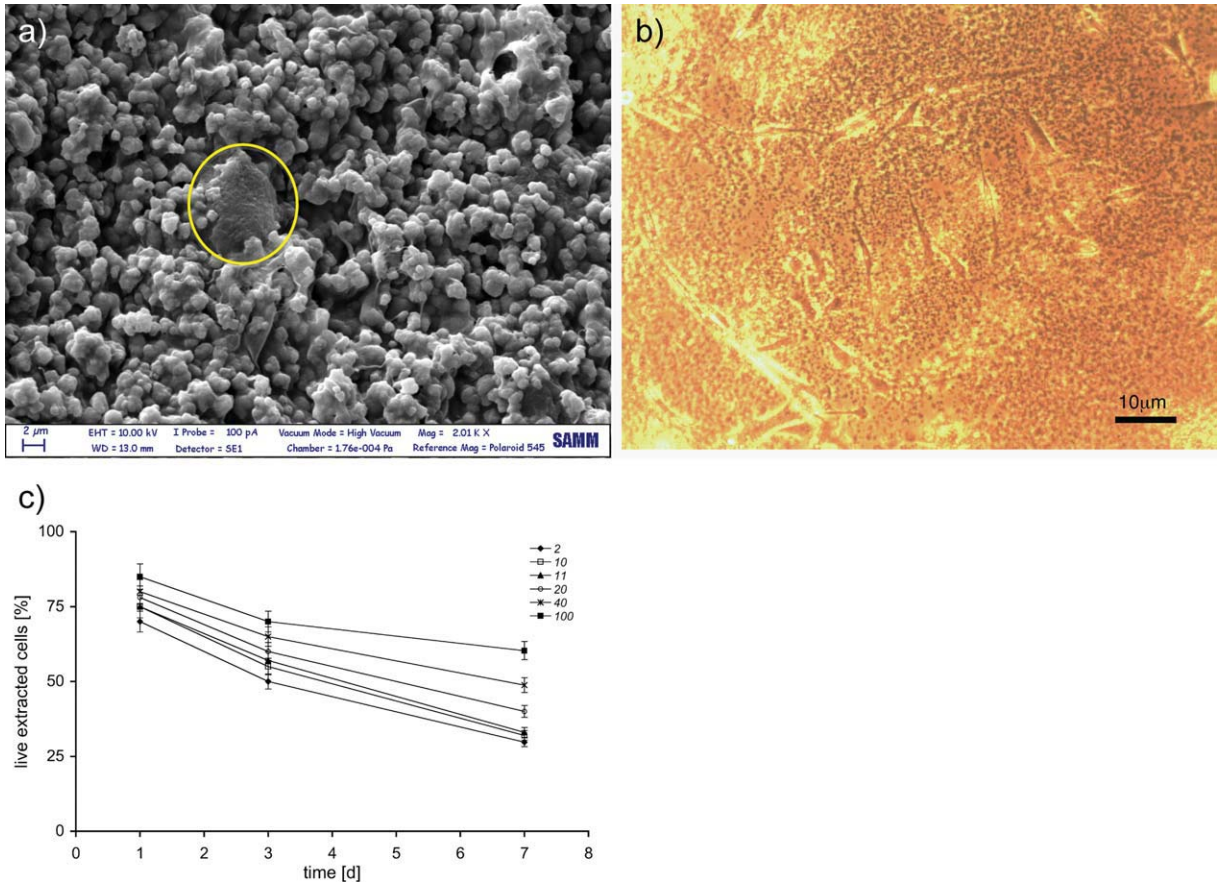

Figure 8 (a) E/SEM image of U87MG cell within AC6 hydrogel matrix at Day 1 (yellow circle); (b) Optical microscopy image showing the U87MG cells morphology at Day 7 included in gel <i>AC6; (c) percentage of live extracted U87MG line cells from hydrogel matrices (*A*/*B* in legend). [Color figure can be viewed in the online issue, which is available at wileyonlinelibrary.com.]

3D cell culture within agarose carbomer hydrogels

Glial cells recently gained very high attention for their potential use in regeneration of damaged CNS tissue[43,44] as far as their neurophysiological role is being more widely understood. Furthermore, glial line cells, i.e., glioma-derived immortalized cells, are commonly used as test cells also because they are also a reference for biocompatibility assessments in materials for CNS applications. Inclusion of glial cells within a hydrogel matrix was shown to be an effective approach for tissue engineering.[45]

Results of cell viability within AC hydrogel samples were presented in Figure 8, where every AC formulations showed ability to carry living cells also after 7 days of encapsulation. This is highly significant, considering that the final aim of these biohybrid systems is not to be growth scaffolds for cell proliferation but to keep cells viable in good percentage and able to proliferate once placed in the target tissue.[23,46] From a qualitative point of view [Fig. 8(a)], the presence of U87MG included inside gel was observed through electron microscopy that evidenced part of cell membrane of emerging U87MG cells within the hydrogel matrix. Moreover, confirmation of such data came from optical microscopy regarding U87MG cells 7 days after hydrogel inclusion [Fig. 8(b)]; cellular elements appear as isolated glial elements with classic shape in a granular matrix due to agarose component of hydrogel. Cell morphology after 1 week of latency is comparable with the ones cultured *in vitro*.

In addition, preliminary cell tests resulted positive in terms of viability [Fig. 8(c)]; at various time points from inclusion, cells were mechanically extracted and the living ones were counted via Trypan Blue live/dead stain.

Moreover, it has to be underlined that the extraction procedure implies the mechanical destruction of the gel matrix and, consequently, this surely results in the killing of several living cells. The counts performed are thus certainly minimum values.[23,26] The quantitative results of the Trypan Blue hematocymetric cell count are presented in Figure 8(c); after 1 week, viability is high, once more in agreement with the literature.[46] The cell culture trend is in

agreement with literature for this kind of devices[46] showing decreasing number of living cells extracted from the polymeric matrix during time and this observation might be mainly due to the difficult permeation of nutrient and oxygen through hydrogel-medium interface.

The key result is that biocompatibility, in terms of living cells after extraction, increases as A/B increases. It is thus possible to claim that a more nanostructured and compact environment is preferred by these cells since it best mimics the extracellular matrix, as expected in an *in vivo* context. Indeed, according to literature, smaller, denser, and nanometer scaled matrices[47] are the most suitable materials for hosting cells for tissue engineering applications because they are best able to mimic their natural environment.

CONCLUSIONS

Using the Flory-Rehner theory, mesh size (ζ), average molecular weight between two following crosslinks (M_C) and crosslinking density (ν) were evaluated, investigating the role of crosslinkers effects on agarose–carbomer library developed for tissue engineering applications. The use of crosslinks with different functionalities, f in Flory notation, underlines the key importance of this parameter in polymer gelation and its contribution was considered where hydroxyl (A) versus carboxyl (B) groups ratio was used as control parameter. On one hand, mesh size and average molecular weight between two following crosslinks showed decreasing trend at increasing A/B values while crosslinking density showed increasing trend. On the other hand, swelling kinetic was studied and again related to A/B ratio; an increasing of crosslinking density in the 3D network, that is also visible from E/SEM analysis, corresponds to a faster swelling kinetic according to the quicker balance between attractive and repulsive forces involved, and *vice versa*. The viscoelastic nature suggested that such hydrogels could be useful as topical materials for cell housing systems. Rheological parameters are indeed among essential issues to build a framework for designing optimal cell housing systems for *in vivo* applications.

In the end, acting on microchemistry of hydrogel library and following a multi scale approach, it was possible to manage macro properties. Moreover, biocompatibility assays confirmed a behavior previously and commonly reported in the literature; nanostructured matrices enhance viability of included cells. Indeed, it was observed that viability increases with the decrease of matrix mesh size. Thus, the smaller the mesh, the better the cell viability.

NOMENCLATURE

M_C	average molecular weight between two following crosslinks (g mol^{-1})
W_t	weight of wet hydrogel (g)
W_d	weight of dry hydrogel (g)
W_s	weight of the swollen hydrogel (g)
Q_V	volumetric swelling ratio (%)
V_1	specific volume of solvent (cm^3 g^{-1})
V_p	specific volume of dry polymer (cm^3 g^{-1})
Q_m	mass swelling ratio (%)
m_i	mass of the ith component (g)
MW_i	molecular weight of the ith component (g mol^{-1})
f_i	functionality of the ith component
A/B	ratio between hydroxyl and carboxyl groups
t^*	time necessary for reach the equilibrium of swelling

Greek symbols

ζ	mesh size (nm)
V	crosslinking density (mol cm^{-3})
χ	interaction parameter between polymer and solvent
τ_c	relaxation time (s)
ω_c	crossover frequency (rad s^{-1})
γ_c	crossover strain (%)

The authors thank Dott. Sacchi for having provided pharmal grade Carbomer 974P. Special thanks to Dr. Hua Wu (ETH Zurich) for his help with the rheological measurements and useful discussions.

References

1. Langer, R. Adv Mater 2009, 21, 3235.
2. Sakurada, K.; McDonald, F. M.; Shimada, F. Angew Chem Int Edit 2008, 47, 5718.
3. Atala, R.; Langer, R.; Thomson, J.; Nerem, R. Principles of Regenerative Medicine; Academic Press: Burlington MA, 2008.
4. Shoichet, M. S. Macromolecules 2010, 43, 581.
5. Ballios, B. G.; Cooke, M. J.; van der Kooy, D.; Shoichet, M. S. Biomaterials 2010, 31, 2555.
6. Liu, Y. X.; Chan-Park, M. B. Biomaterials 2010, 31, 1158.
7. Wan, A. C. A.; Ying, J. Y. Adv Drug Deliv Rev 2010, 62, 731.
8. Dumitriu, S. Polymeric Biomaterials, 2nd ed.; Marcel Dekker: New York, 2002.
9. Engel, E.; Michiardi, A.; Navarro, M.; Lacroix, D.; Planell, J. A. Trends Biotechnol 2008, 26, 39.
10. Slaughter, B. V.; Khurshid, S. S.; Fisher, O. Z.; Khademhosseini, A.; Peppas, N. A. Adv Mater 2009, 21, 3307.
11. Peppas, N. A. Hydrogels in Medicine and Pharmacy; CRC Press: Boca Raton, FL, 1987.
12. Santoro, M.; Marchetti, P.; Rossi, F.; Perale, G.; Castiglione, F.; Mele, A.; Masi, M. J Phys Chem B 2011, 115, 2503.
13. Baumann, M. D.; Kang, C. E.; Tator, C. H.; Shoichet, M. S. Biomaterials 2010, 31, 7631.
14. Kim, Y. T.; Caldwell, J. M.; Bellamkonda, R. V. Biomaterials 2009, 30, 2582.
15. Yu, L.; Ding, J. D. Chem Soc Rev 2008, 37, 1473.

16. Flory, P. J. Principles of Polymer Chemistry; Cornell University Press: New York, 1953.
17. Metters, A.; Hubbell, J. Biomacromolecules 2005, 6, 290.
18. Hynes, S. R.; Rauch, M. F.; Bertram, J. P.; Lavik, E. B. J Biomed Mater Res A 2009, 89A, 499.
19. Urquhart, A. J.; Anderson, D. G.; Taylor, M.; Alexander, M. R.; Langer, R.; Davies, M. C. Adv Mater 2007, 19, 2486.
20. Balgude, A. P.; Yu, X.; Szymanski, A.; Bellamkonda, R. V. Biomaterials 2001, 22, 1077.
21. Jones, D. S.; Bruschi, M. L.; de Freitas, O.; Gremiao, M. P. D.; Lara, E. H. G.; Andrews, G. P. Int J Pharm 2009, 372, 49.
22. Nguyen, M. K.; Lee, D. S. Macromol Biosci 2010, 10, 563.
23. Perale, G.; Giordano, C.; Bianco, F.; Rossi, F.; Daniele, F.; Tunesi, M.; Crivelli, F.; Matteoli, M.; Masi, M. Int J Artif Organs 2011, 34, 295.
24. Tunesi, M.; Rossi, F.; Daniele, F.; Bossio, C.; Perale, G.; Bianco, F.; Matteoli, M.; Giordano, C.; Cigada, A. Regen Med 2009, 4, S295.
25. Perale, G.; Veglianese, P.; Rossi, F.; Peviani, M.; Santoro, M.; Llupi, D.; Micotti, E.; Forloni, G.; Masi, M. Mater Lett 2011, 65, 1688.
26. Rossi, F.; Perale, G.; Masi, M. Chem Pap 2010, 64, 573.
27. Kretschmann, O.; Schmitz, S.; Ritter, H. Macromol Rapid Commun 2007, 28, 1265.
28. Zhao, Q.; Sun, J. Z.; Ling, Q. C.; Zhou, Q. Y. Langmuir 2009, 25, 3249.
29. Rossi, F.; Santoro, M.; Casalini, T.; Veglianese, P.; Masi, M.; Perale, G. Int J Mol Sci 2011, 12, 3394.
30. Begam, T.; Tomar, R. S.; Nagpal, A. K.; Singhal, R. J Appl Polym Sci 2004, 94, 40.
31. Begam, T.; Nagpal, A. K.; Singhal, R. J Appl Polym Sci 2003, 89, 779.
32. Hu, B. H.; Su, J.; Messersmith, P. B. Biomacromolecules 2009, 10, 2194.
33. van de Manakker, F.; Vermonden, T.; el Morabit, N.; van Nostrum, C. F.; Hennink, W. E. Langmuir 2008, 24, 12559.
34. Brandrup, J. Polymer Handbook, 4th ed.; Wiley: New York, 2003.
35. Huang, J. C. J Appl Polym Sci 2010, 119, 719.
36. Huglin, M. B.; Rehab, M. M. A. M.; Zakaria, M. B. Macromolecules 1986, 19, 2986.
37. de Jong, S. J.; van Eerdenbrugh, B.; van Nostrum, C. F.; Kettenes-van de Bosch, J. J.; Hennink, W. E. J Control Release 2001, 71, 261.
38. Cleland, R. Biopolymers 1970, 9, 811.
39. Rammensee, S.; Huemmerich, D.; Hermanson, K. D.; Scheibel, T.; Bausch, A. R. Appl Phys A Mater 2006, 82, 261.
40. Katsares, V.; Petsa, A.; Felesakis, A.; Paparidis, Z.; Nikolaidou, E.; Gargani, S.; Karvounidou, I.; Ardelean, K. A.; Grigoriadis, N.; Grigoriadis, J. Lab Med 2009, 40, 557.
41. Tan, H. P.; Chu, C. R.; Payne, K. A.; Marra, K. G. Biomaterials 2009, 30, 2499.
42. Barreiro-Iglesias, R.; Alvarez-Lorenzo, C.; Concheiro, A. J Control Release 2001, 77, 59.
43. Blakemore, W. F.; Franklin, R. J. M. Trends Neurosci 1991, 14, 323.
44. Bacaj, T.; Tevlin, M.; Lu, Y.; Shaham, S. Science 2008, 322, 744.
45. Perale, G.; Bianco, F.; Giordano, C.; Matteoli, M.; Masi, M.; Cigada, A. J Appl Biomater Biomech 2008, 6, 1.
46. Brannvall, K.; Bergman, K.; Wallenquist, U.; Svahn, S.; Bowden, T.; Hilborn, J.; Forsberg-Nilsson, K. J Neurosci Res 2007, 85, 2138.
47. Flemming, R. G.; Murphy, C. J.; Abrams, G. A.; Goodman, S. L.; Nealey, P. F. Biomaterials 1999, 20, 573.